Journal of Controlled Release 209 (2015) 238–247

Contents lists available at ScienceDirect

Journal of Controlled Release

journal homepage: www.elsevier.com/locate/jconrel

PEG shielded MMP sensitive CPPs for efficient and tumor specific gene delivery in vivo

Kadi-Liis Veiman [a,*], Kadri Künnapuu [a], Tõnis Lehto [a,b], Kristina Kiisholts [a], Kalle Pärn [a], Ülo Langel [a,b], Kaido Kurrikoff [a]

[a] Laboratory of Molecular Biotechnology, Institute of Technology, University of Tartu, Nooruse 1, 50411 Tartu, Estonia
[b] Department of Neurochemistry, The Arrhenius Laboratories for Natural Sciences, Stockholm University, SE-10691 Stockholm, Sweden

ARTICLE INFO

Article history:
Received 8 January 2015
Received in revised form 24 April 2015
Accepted 27 April 2015
Available online 30 April 2015

Keywords:
Gene delivery
Tumor
PEGylation
Cell-penetrating peptide
Non-covalent complexes
Matrix metalloprotease

ABSTRACT

Gene therapy has great potential to treat a range of different diseases, such as cancer. For that therapeutic gene can be inserted into a plasmid vector and delivered specifically to tumor cells. The most frequently used applications utilize lipoplex and polyplex approaches where DNA is non-covalently condensed into nanoparticles. However, lack of in vivo efficacy is the major concern that hinders translation of such gene therapeutic applications into clinics. In this work we introduce a novel method for in vivo delivery of plasmid DNA (pDNA) and efficient tumor-specific gene induction using intravenous (i.v) administration route. To achieve this, we utilize a cell penetrating peptide (CPP), PepFect14 (PF14), double functionalized with polyethylene glycol (PEG) and a matrix metalloprotease (MMP) substrate. We show that this delivery vector effectively forms nanoparticles, where the condensed CPP and pDNA are shielded by the PEG, in an MMP-reversible manner. Administration of the complexes results in efficient induction of gene expression specifically in tumors, avoiding normal tissues. This strategy is a potent gene delivery platform that can be used for tumor-specific induction of a therapeutic gene.

1. Introduction

Gene therapy has great potential to treat a wide range of different diseases which occur due to defective gene expression levels, such as in many types of cancer. The most common way to implement gene therapy is to deliver therapeutic genetic material into cells to reestablish protein levels by restoring or altering gene expression. However, delivery of nucleic acid-based biomolecules remains prohibitively challenging and efficient, tunable/controllable [1] and non-toxic [2] delivery vectors are required. In addition to gene transfer efficiency, the delivery to tumor cells also requires tissue specificity. Nucleic acids have been delivered to cells via different non-viral vectors; most common examples are lipoplexes and polyplexes [3]. All these are efficient delivery agents in cell cultures but translating them for in vivo applications usually lose their effectiveness and even if ability to deliver genes is maintained, additional modifications are needed to gain tissue specificity [4,5].

One potential class of delivery vectors are cell penetrating peptides (CPPs) [6] which can be used to non-covalently condense nucleic acids into nanoparticles [7,8] and deliver them into cells. The first successful in vivo gene delivery using CPP and i.v. route was demonstrated in 2002, although the efficacies were slightly lower than with liposomes or PEI and the effects were associated with some toxicity [9]. Accordingly, gene delivery vector has to possess high efficacy and low toxicity, plus an additional mechanism for achieving tumor-specificity. One of the most advanced CPP vector for tumor-specific delivery of cargo for in vivo applications was proposed by R. Tsien's research group, where the cell penetration activity is initially masked by an anionic peptide domain and could be reactivated via tumor-selective cleavage by matrix metalloproteases (MMPs) [10]. Matrix metalloproteinase 2 is a protease engaged in the breakdown of extracellular matrix components that is required for neoplastic growth and it is overexpressed in almost all types of tumors, therefore being a marker of malignancy [11]. In the current report we have combined a non-covalent CPP/nucleic acid complexation strategy with similar CPP-shielding and tumor-specific activation as described above. In this case, CPP is not deactivated through an anionic domain, because this would interfere with the CPP/nucleic acid complex formation. Instead, we use polyethylene glycol (PEG), which serves several purposes at the same time. First, PEG in the outer layer of the nanoparticles is a biologically inert shield that inhibits contacts with cell membranes, thereby masking the CPP activity [12], a property that can later be restored in an MMP-sensitive

Abbreviations: CPP, cell-penetrating peptide; CR, charge ratio; DLS, dynamic light scattering; EPR, enhanced permeability and retention effect; EtBr, ethidium bromide; MMP, matrix metalloproteases; MPS, mononuclear phagocyte system; N2a, Neuro2a cells; ON, oligonucleotide; pDNA, plasmid DNA; PEG, polyethylene glycol; PF14, PepFect14; pLuc2, luciferase encoding plasmid; RLU, relative light unit.

* Corresponding author at: Institute of Technology, University of Tartu, Tartu 50411, Estonia.
E-mail address: kadi-liis.veiman@ut.ee (K.-L. Veiman).

http://dx.doi.org/10.1016/j.jconrel.2015.04.038

manner. Second, PEG is able to prolong the half-life of therapeutic molecules in the bloodstream by postponing recognition by the mononuclear phagocyte system (MPS) and preventing the interactions with blood components. Secondary to the abovementioned, PEGylation also enhances passive tumor targeting using the enhanced permeability and retention (EPR) effect [13]. In this work we apply efficient gene delivery properties of PepFect14 [14] to induce high and specific gene expression levels in tumor tissue thorough reversible inactivation strategy. We show that using this method, efficient and tumor-selective gene induction is achieved.

2. Material and methods

2.1. Synthesis of peptides

All peptides were synthesized in a stepwise manner in a 0.1 mmol scale on an automated peptide synthesizer (Applied Biosystems, ABI433A) by using standard protocols for Fmoc solid-phase synthesis. Rink-amide MBHA resin (Orpegen, Germany) was used as the solid phase to obtain C-terminally amidated peptides. N-terminally stearylated peptides were prepared by treatment of peptidyl resin with 4 equiv. of stearic acid (Sigma-Aldrich), 4 equiv. of HOBt/HBTU (MultiSynTech), and 8 equiv. of DIEA (Sigma-Aldrich) in DMF/DCM for 18 h. C-terminally PEGylated peptides were prepared by treatment of Rink-amide MBHA resin with 2 equiv. of Fmoc-PEG_n-CH_2CH_2COOH (PEG1000, PEG2000 — JenKem, USA, PEG600 — Chempep, USA), 2 equiv. of HOBt/HBTU and 4 equiv. of DIEA in DMF/DCM for 24 h which was followed by standard Fmoc peptide synthesis. The final cleavage was performed using a standard protocol [95% trifluoroacetic acid (TFA)/2.5% TIS/2.5% water] for 2 h at room temperature. Peptides were purified by RP-HPLC using a C3 column and 5–80% acetonitrile (0.1% TFA) gradient. Molecular weight of the peptides was analyzed by MALDI-TOF mass-spectrometry, and purities were >90% as determined by analytical HPLC.

2.2. Complex formation

For complex formation, stability and cell culture assays 0.5 μg of pLuc2 plasmid was mixed with CPPs at different peptide:pDNA charge ratios (CR) in MQ water in 50 μl (1/10th of the final treatment volume). CRs were calculated theoretically, taking into account the positive charges of the peptide and negative charges of the pDNA. In order to form complexes at different PEGylation rates, PEGylated peptide was firstly mixed with pDNA and thereupon PF14 was added and complexes were formed by incubating 40 min at room temperature. PEGylation rate is defined as the amount of PF14 which is substituted with its PEGylated PF14 analog, for example, PEGylation rate 20% represents complexes with 80% of PF14 and 20% corresponds to PEGylated PF14 analog.

For in vivo studies 20 μg of pLuc2 per animal (0.8 mg/kg) was mixed with 1 mM peptide at CR2 or CR4 in MQ water and the volume of complexes was kept constantly at 100 μl. For PEGylated complexes, first CPP-PEG was mixed with pDNA in MQ water and incubated for 5 min followed by addition of parent CPP. After 40 min of incubation 100 μl of 10% glucose was added to preformed complexes and immediately injected intravenously via tail vein.

2.3. Gel shift and EtBr exclusion assay

pDNA condensation and incorporation into complexes was analyzed using a gel shift assay and ethidium bromide (EtBr) (Sigma, Sweden) exclusion assay. Briefly, for both assays, complexes were formed as described above. For gel shift assay, samples were electrophoresed on agarose gel (1%) in TAE (1×) and imaged by staining the gel with EtBr (0.5 μg/ml). Gels were visualized using the UVIpro Gold Gel Documentation System (United Kingdom). In the EtBr exclusion assay, after 40 min. of incubation, 165 μl of MQ water was added to each complex sample (20 μl) and transferred into a black 96-well plate (NUNC, Sweden). Thereafter, 15 μl (5.33 μg/ml) of EtBr solution was added to give a final EtBr concentration of 400 nM. After 15 min, the fluorescence was measured on a Spectra Max Gemini XS fluorometer (Molecular Devices, Palo Alto, CA) at $\lambda_{ex} = 518$ nm and $\lambda_{em} = 605$ nm. Results are expressed as relative fluorescence and a value of 100% is attributed to the fluorescence of naked pDNA with EtBr.

2.4. Heparin displacement assay

For the analysis of peptide/pDNA or peptide/Cy5-labeled pDNA complexes resistance to heparin, preformed peptide/pDNA complexes containing 100 ng of plasmid DNA were incubated for 30 min at 37 °C in the presence of heparin sodium (Sigma-Aldrich, Germany) over a range of concentrations. After the incubation period, reactions were analyzed by EtBr exclusion assay or by gel shift assay which are described above. Results are expressed as relative fluorescence, where 100% is the fluorescence of naked pDNA

2.5. Enzymatic stability

The resistance against degradative enzymes such as proteases and nucleases was evaluated using fetal bovine serum (FBS, Life Technologies, USA) and DNase I (Thermo Scientific, USA). For serum stability assay, complexes were formed as described above and 10% of FBS was added to complexes and as a control accordingly the same amount of MQ water was added to complexes. Thereafter complexes were incubated for 2 or 4 h at 37 °C and then analyzed by gel shift assay (described above) or used for transfection as described in plasmid delivery section. In the case of nuclease stability assay, 12.5 μl of DNase I in buffer (as instructed in the protocol by the manufacturer) or same amount of buffer alone was added to complexes (1.05 μg pDNA dose at CR2 or CR4, DNase final concentration was 0.02 U/μl). Treatment was carried out for 30 min. at 37 °C and thereafter complexes were analyzed by gel shift assay and used for plasmid delivery assay described in plasmid delivery assay section. In order to visualize degradation of pDNA, proteinase K treatment was carried out. Complexes or naked pDNA were incubated with 20 μg of proteinase K (Thermo Scientific, USA) for 30 min at 37 °C and thereafter analyzed by gel shift assay.

2.6. Dynamic light scattering (DLS) measurements

Hydrodynamic mean diameter of the DNA nanoparticles was determined by dynamic light scattering studies using a Zetasizer Nano ZS apparatus (Malvern Instruments, United Kingdom). Peptide/pDNA complexes were formulated according to the protocol for in vitro transfection, as described above, and assessed in disposable low volume cuvettes. Briefly, pDNA complexes were formulated in MQ water, in 100 μl volume, at a final concentration of 0.01 μg/μl of pDNA. After 40 min of incubation at room temperature complexes were measured or glucose (final concentration 5%) was added. Measurements were performed at over a period of time and at RT, for each sample ($n = 2$) 3 measurements were made and 1 measurement was set to 10 runs (1 run was 10 s). For zeta potential measurements pDNA complexes were formulated in MQ water, in 300 μl volume, at a final concentration of 0.01 μg/μl of pDNA. After 40 min incubation at room temperature, the complexes were diluted in MQ or glucose (final concentration 5%) into a final volume of 1 ml. Measurements were performed at over a period of time and at RT, for each sample ($n = 1–2$) 3 measurements were made and 1 measurement was set to 10 runs.

2.7. Cell culture

CHO cells were grown in humidified environment at 37 °C, 5% CO_2 and cultivated in Dulbecco's Modified Eagle's Medium F12 (DMEM-

F12) with glutamax supplement with 0.1 mM non-essential amino acids, 1.0 mM sodium pyruvate, 10% FBS, 100 U/ml penicillin and 100 μg/ml streptomycin (PAA Laboratories GmbH, Germany). U87 and Neuro2a and cells were grown in humidified environment at 37 °C, 5% CO_2 and cultivated in DMEM with glutamax supplemented with 0.1 mM non-essential amino acids, 1.0 mM sodium pyruvate, 10% FBS, 100 U/ml penicillin and 100 μg/ml streptomycin.

2.8. Plasmid delivery assay

4×10^4 CHO or 5×10^4 U87 cells or 3×10^4 Neuro2a cells were seeded 24 h before experiment into 24-well plates. Cells were treated with peptide/pDNA complexes at CR2 or CR4 for 4 h in serum containing media, followed by addition of 1 ml 10% serum containing medium and incubated for another 20 h. Thereafter, cells were lysed using 100 μl 0.1% Triton X-100 in PBS for 15 min at 4 °C. Luciferase activity was measured using Promega's luciferase assay system according to the manufacturer's protocol on GLOMAX™ 96 microplate luminometer (Promega, Sweden) and normalized to protein content (BioRad Protein Assay, USA).

To study the effect of MMP2 cleavage to transfection efficiency, peptide/pDNA complexes were preincubated with an active recombinant MMP2 (0.1 mg/ml, Calbiochem, Germany) for 30 min at 37 °C and then proceeded with transfection as described above. Thereafter, cells were washed with 1 × PBS and lysed as described above. Luciferase activity was measured and normalized to protein content.

2.9. Cell proliferation assay

Cell proliferation was studied with MTS proliferation assay (Promega, Sweden). Briefly, 1×10^4 cells were seeded 1 day before treatment into a 96-well plate (Greiner Bio One, Germany). Cells were treated with peptide/pDNA complexes at CR2 and with different PEGylation rate;, however, to optimize the amounts to fit a 96-well format, 5 times less pDNA and peptide in MQ water was used compared to 24-well plates. After 4 h fresh media (200 μl) was added and 24 h later MTS reagent was added and absorbance was measured after 2 h of incubation with Tecan Sunrise microplate reader (Tecan Trading AG, Switzerland). Untreated or pDNA-treated cells were defined as 100% viable.

2.10. Tumor induction

All animal experiments and procedures were approved by the Estonian Laboratory Animal Ethics Committee (approval nos. 69 and 70, dated Feb 9, 2011).

The mouse Neuro2a tumors were induced in BALB/c mice subcutaneously (s.c.). Human tumor xenografts were induced in nude animals (Hsd: Athymic Nude-Foxn1nu female, 4–6 week old, Harlan, UK). The tumors were induced by resuspending 1×10^6 cells in 100 μl volume

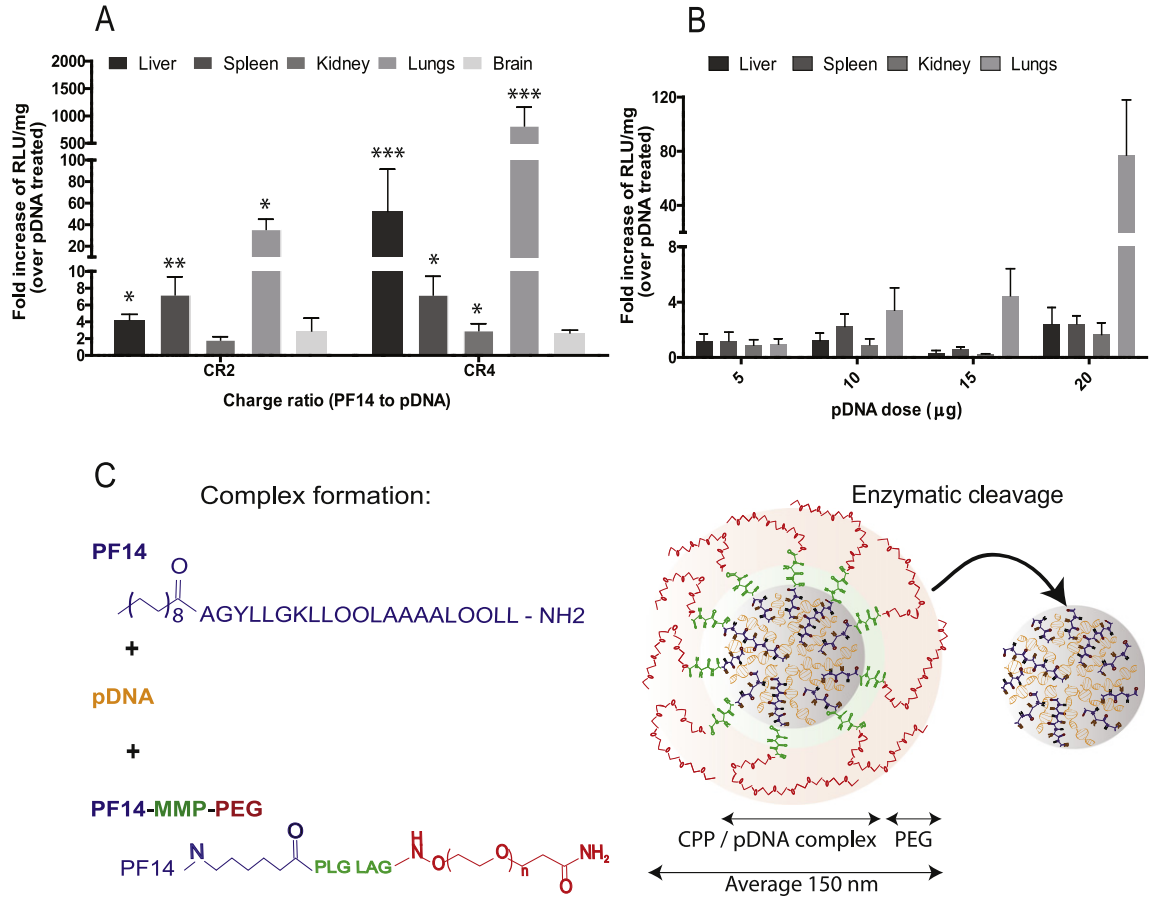

Fig. 1. Biological activity of PF14 in vivo in different tissues. (A) The ability of PF14/pDNA complexes to induce gene expression levels in different tissues was evaluated in vivo. Complexes with 20 μg of pLuc2 plasmid were administered intravenously via the tail vein. After 24 h, tissues were harvested, homogenized, and lysed. Thereafter, luciferase activity was measured and normalized to the protein content. Values are represented as fold increase of RLU/mg over the pDNA treated group. Stars represent p-values from Kruskal–Wallis comparison of RLU values of CR2 and CR4 against pDNA group. *$p < .05$, **$p < .01$, ***$p < .001$. $N = 6–10$ in each group. (B) To evaluate the ability of complexes to induce gene expression at different pDNA doses, complexes were mixed at CR4, using 5–20 μg of pLuc2 plasmid. $N = 2–4$ in each group. (C) The schematic construction principle of a tumor-targeted CPP/nucleic acid nanocomplex. The parent CPP, PF14 was C-terminally modified with PEG using an MMP2-sensitive peptide linker between the CPP and PEG moieties. Hypothetically, the core of the complex consists of the cationic CPP (PF14) and anionic DNA. A proportion of the CPP is substituted to PEGylated CPP, and, according to our hypothesis, PEG orients itself as an outer shell which provides a neutral shield that inhibits transfection until cleaved by a tumor-specific MMP2. After this an active particle is generated.

of ice-cold DMEM without any supplements. The xenografting was performed by implanting the cell suspension subcutaneously to the right flank. At the appearance of the first signs of tumor growth (for the subcutaneous tumors, tumor size of approximately 100 mm^3), mice were injected i.v. (via tail vein) with the peptide/pDNA complexes.

2.11. Quantitation of luciferase levels and fluorescence from tissues

24 h after administration of complexes the mice were sacrificed using cervical dislocation and tissues were harvested and snap-frozen on dry ice. The tissues were homogenized using Precellys®24-Dual homogenization system (Bertin Technologies, France) and lysed using 1 × Promega lysis buffer (Promega, Sweden). Luciferase content was analyzed as described previously [15]. Briefly, homogenized tissues were thawed and 500 μl of Promega Reporter lysis 1 × buffer was added. The samples were subsequently vortexed for 15 min, subjected to 3 consecutive freeze–thaw cycles (liquid nitrogen and 37 °C water bath), centrifuged for 3 min at 10 000 g, 4 °C; supernatant removed and saved for later analysis. 500 μl of lysis buffer was again added to the pellet and the extraction process repeated (without freeze–thaw cycles). The second supernatant was combined with the first one and was subjected to luciferase activity assay or for fluorescence measurements. Firstly, luciferase was measured with Promega luciferase assay system, in combination with GLOMAX 96 microplate luminometer (Promega, Sweden). Accordingly, 20 μl of the supernatant was transferred to the white 96-well plate and 80 μl of luciferase substrate was added to each sample. An average LU (light unit) out of 3 technical replicates was used for data analysis. The LU values within each sample were normalized to protein content (BioRad, United States) and the resultant RLU/mg were normalized to the corresponding tissue of the animals that received naked pDNA injection (sham treatment). For Cy5-labeled pDNA fluorescence measurements 100 μl of samples were transferred to black 96-well plate (NUNC, Sweden). Then, the fluorescence was measured on a Spectra Max Gemini XS fluorometer (Molecular Devices, Palo Alto, CA) at $\lambda_{ex} = 650$ nm and $\lambda_{em} = 670$ nm. An average FU (fluorescence unit) out of 3 technical replicates was used for data analysis. The FU values within each sample were normalized to protein content (BioRad, United States) to get RFU/mg.

2.12. Quantitation of fluorescence from blood

Complex stability in blood was studied using Cy5-labeled pDNA (Mirus, USA), where 20 μg labeled pDNA was mixed with the peptides and injected as described above. Blood was collected at different time points (0,5 h–6 h) from saphenous vein using sodium-heparinized (80 iu/ml ± 30%) capillaries (Marienfeld, Germany;, thereafter, blood was transferred to heparinized blood collecting tubes (Sarstedt, Germany) and stored at −20 °C until the analysis. Then 20 μl of blood was transferred to a black 96-well plate and the sample was diluted 5 times in MQ water. Cy5-pDNA fluorescence was measured on a Spectra Max Gemini XS fluorometer (Molecular Devices, Palo Alto, CA) at $\lambda_{ex} = 650$ nm and $\lambda_{em} = 670$ nm and the fluorescence of untreated sample was subtracted. Acquired values were normalized to pDNA concentration which was calculated based on naked pDNA or peptide/pDNA complex calibration curves.

3. Results and discussion

3.1. Optimizing PF14 / pDNA formulations for in vivo use

We have shown earlier that PF14 is an efficient gene transport vector in cell cultures [14] but its gene delivery potential has not yet been evaluated in vivo conditions. To test this we complexed peptide with a pluc2 gene expressing vector and administered systemically via intravenous (i.v.) administration route. PF14-mediated gene delivery induces luciferase expression in various organs, particularly in lungs, where luciferase levels reach up to 3 logs over control (naked pDNA) levels (Fig. 1A). However, we occasionally observed acute toxic reactions occurring with PF14/pDNA (20 μg dose) at CR4, where about 1 out of 15 animals died within 10 min after injection. We hypothesize that the complexes of PF14 may aggregate upon contact with blood, as shown earlier with cationic liposome/pDNA [16] or with polyplex/pDNA [17]. This suggests that some factors during the formation of complexes need to be addressed to achieve their potential for use in vivo. When comparing different charge ratios, CR4 is more efficient than CR2, an effect that is especially apparent in the lungs and liver. In addition, the minimal effective dose of pDNA is 20 μg per animal (0.8 mg/kg) (Fig. 1B).

Table 1
Peptides sequences and the modifications used.

Name	Construction principle	Sequence
PepFect14		
PepFect141	PF14-PEG600 (1)	
PepFect142	PF14-PEG1000 (2)	
PepFect143	PF14-PEG2000 (2)	
PepFect144	PF14-MMP2-PEG600	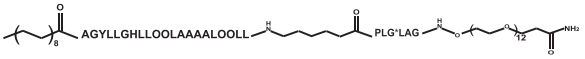
PepFect145	PF14-MMP2-PEG1000	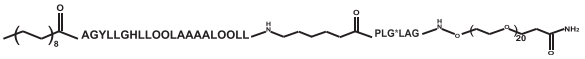
PepFect146	PF14-MMP2-PEG2000	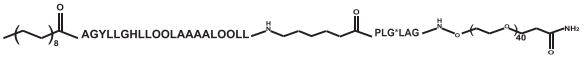
PepFect147	PF14-scrMMP2-PEG600	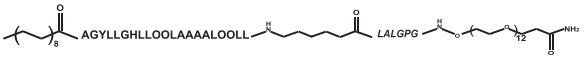
PepFect148	PF14-scrMMP2-PEG1000	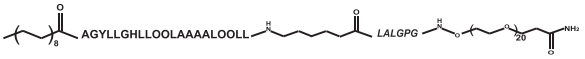
PepFect149	PF14-scrMMP2-PEG2000	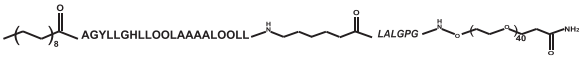

(1) Monodisperse PEG, PEG size indicated by the molecular mass.
(2) Polydisperse PEG, PEG size indicated by the average molecular mass.

3.2. Optimization of PEG-functionalized complexes for gene delivery

3.2.1. Characterization of PEGylated peptide/pDNA complexes

We next intended to explore the possibility of using PEG as a shield to inactivate the CPP activity, because PEGylation has the potential to increase general in vivo usability by inhibiting unwanted contacts with blood proteins and cells. To functionalize PF14 with PEG, a series of PF14 analogs were synthesized, where PEG with 3 different chain lengths (PEG600, PEG1000 and PEG2000) was covalently conjugated to the C-terminus (Table 1, Fig. 1C). We named these PF141, PF142 and PF143, respectively. Our hypothesis was that the functionalized PF14 would still retain the complex formation ability with the core of the particle being formed by the cationic peptide and anionic DNA and the PEG would orient itself as an outer shell and act as a moiety that would mask the transfection ability of CPP. Later, delivery can be restored only to specific tissues in a controllable manner. Accordingly, the two crucial questions for us were: can the complexes be formed and does the PEG form an outer shell?

We first assessed the ability of PEGylated peptides to form stable complexes with pDNA. For that, we carried out a gel shift assay where the PEGylated peptides (PF141, PF142 and PF143, Table 1) were complexed with pDNA. Not surprisingly, incorporation of pDNA into complexes occurred in a CR-dependent manner: more incorporation was observed at higher CR, whereas in the case of PF143 all pDNAs were incorporated into complexes already at CR1 (Fig. S1A), yet a CR4 was required for PF142 (Fig. S3); the other peptides fell in between these two extremes (Figs. 2A, S2A). Similar results could be seen in pDNA condensation studies with an EtBr exclusion assay where the quenching of the fluorescence was analyzed. Complexes with PF143 showed the highest quenching of EtBr (the plateau is reached already at CR1, Fig. S1B), whereas PF14 and PF141 reached the plateau at CR2 and CR3 (Figs. 2B, S2B). PF142 formed less condensed complexes (Fig. S3B).

3.2.2. Formulation of complexes with mixed CPP and CPP-PEG

Hypothetically, more favorable therapeutic properties may be achieved with complexes that have adjustable amounts of PEG; therefore, we were interested in modifying the functionalization rate of complexes and for that we tested an alternative approach, where a proportion of the CPP-PEG would be substituted with the parent

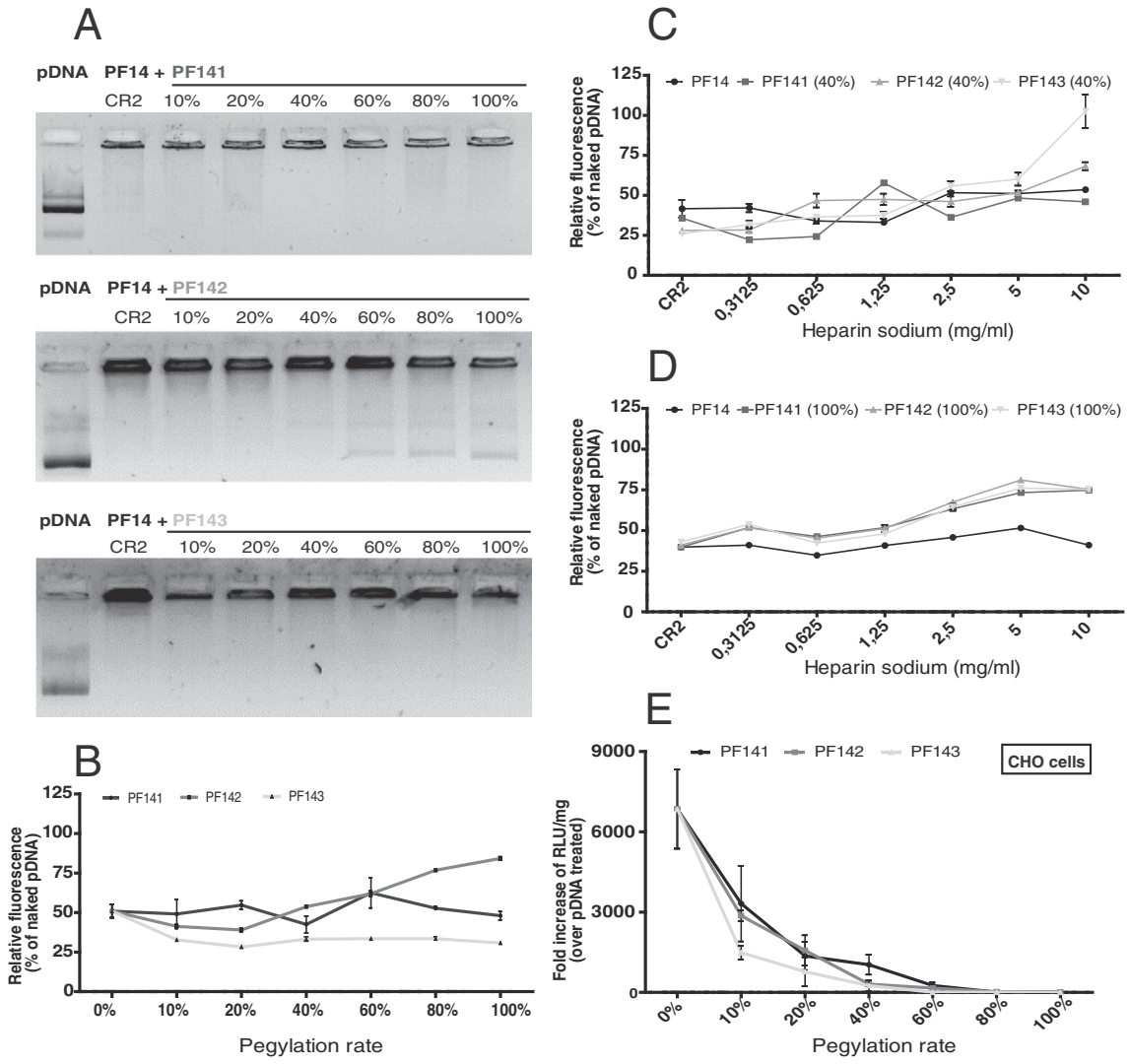

Fig. 2. The ability of PEGylated peptides to form complexes with pDNA and transfect cells at CR2. (A) Complex formation at increasing range of PEGylation rate was assessed with a gel shift assay. (B) The ability of PEGylated peptides to condense pDNA was evaluated using an EtBr exclusion assay. PEGylation rate 0% represents PF14/pDNA complexes formed at CR2. Results are represented as relative fluorescence, where 100% is the fluorescence of naked pDNA. A heparin displacement assay was used to analyze the stability and dissociation profile of PEGylated complexes at PEGylation rate 40% (C) and 100% PEGylated complexes (D). Results are represented as relative fluorescence with EtBr, where 100% is naked pDNA fluorescence. (E) Transfection efficiency of PF141, PF142 and PF143 and pDNA complexes were evaluated in CHO cells at CR2 and at different PEGylation rates. For that luciferase encoding pDNA was delivered and after 24 h luciferase activity was measured and normalized against protein content. Results are represented as fold increase of RLU/mg over naked pDNA treated cells.

peptide, thereby yielding a CPP/pDNA complex with the desired functionalization rate (Fig. 1C). We prepared a series of complexes, consisting of 3 different components: CPP, CPP-PEG and pDNA, and titrated the ratio of CPP to CPP-PEG. To characterize the amount of PEGylated peptide containing within the complexes, we use the term PEGylation rate, which is defined as the amount of PF14 that is substituted with its PEGylated analog. For example, a PEGylation rate of 20% means that 20% of the cationic charges arise from the PEGylated peptide.

Importantly, we observed that complexes formed with CPP and CPP-PEG incorporated and condensed pDNA. At lower CR, a higher PEGylation rate correlated with lower pDNA incorporation and condensation. Curiously, complexes with PF142 (PEG1000) tended to be less condensed (Fig. S3B) and less pDNA (Fig. 2A) was incorporated into complexes. PF141 and PF143 fully incorporated pDNA starting from CR2, although PF143 formed more condensed complexes already at lower CRs (Fig. 2A and B). This indicates that a lower concentration of PF143 is required to condense the same amount of pDNA, while PF141 complexes, at least at higher PEGylation rates, are not able to condense pDNA as efficiently. PF142 fully incorporates pDNA only at higher CR, and even then the complexes remain loose, which is surprising considering that complexes with the smallest and the largest PEGs (PEG600 and PEG2000) appear to be more condensed than with the middle-sized PEG (PEG1000). We hypothesize that PEG600 in PF141 is small enough to be incorporated into the complex core to a small extent, resulting in more loose interactions between cationic CPP and anionic pDNA. In contrast, PF142 is able to incorporate pDNA into complexes only at lower PEGylation rates, when increasing the PEGylated peptide content, a free pDNA fraction is observed (Fig. 2A). It may be that PEG1000 in PF142 at high PEGylation rate complexes may also be incorporated into the particle core to a small extent; however, PEG1000 is large enough to prevent complex formation in these situations. Therefore, it seems that in the case of PEG600 and PEG1000, complex stability largely depends on PEGylation rate, where increasing the proportion of PEG gradually destabilizes the complex. PEG2000 in PF143 on the other hand is large enough that it forms a stable outer PEG layer, yielding the most condensed complexes.

To compare the strength of complexes we used a heparin displacement assay [7]. Accordingly, the PEG-functionalized complexes were weaker than parent PF14/pDNA complexes at CR2 (Fig. 2D). When increasing the CR to 4, differences between the PEG sizes during complex formation become apparent: complexes with PF143 possessed the weakest pDNA complexation ability, while PF141 and PF142 formed stronger complexes (Fig. S3D). To understand to what degree the PEGylation rate alters the stability of the complexes, we analyzed PF14/PF14-PEG complexes. PF14 and its analogs PF142 and PF143 with a PEGylation rate of 40% formed similarly condensed nanocomplexes at CR2 and CR4 (Figs. 2C and S3C). Therefore, heparin treatment was carried out using those conditions. We saw that PF142 at CR2 forms more similar complexes to PF14 than PF143, where the latter forms weaker complexes (Fig. 2C). Overall, mixing the parent peptide with PEGylated peptides increases the stability of PEGylated complexes and at CR4, a higher concentration of heparin was required to partially release pDNA (Fig. S3C).

To determine the PEGylated peptide/pDNA complex size and surface charge DLS measurements were carried out. All PEGylated peptide/pDNA complexes remained in the range of 100–200 nm (Table S1) and displayed positive surface charge between 28 and 48 mV (Table S2). It appeared that complexation of pDNA with peptide carrying a higher molecular weight PEG (PF143, PF146 and PF149), a slight shift of surface charge occurring from about 45 to 30 mV. Peptides carrying smaller PEGs did not have significant change in surface charge. Adding glucose (final concentration 5%) to preformed complexes increased heterogeneity and the average size of PEGylated complexes increased to 150–250 nm (Table S1). No significant differences between peptides carrying increasing PEG chains were observed. This could indicate that higher molecular weight PEG chains are needed to make complexes more homogenous [18]. Intriguingly, adding glucose to complexes turned zeta potential more neutral, but overall surface charge remained positive. The results also suggest that increasing PEGylation rate turned the surface charge more neutral in the presence of glucose. For example, 100% of PF141 in MQ water had surface charge 41 mV, but in the presence of glucose it shifted to 17 mV, reducing almost two times, an effect which could be seen in the case of other PEGylated peptide/pDNA complexes as well (Table S2).

Because our initial goal was to shield transfection properties of PF14 using PEG, we studied the effect of PEGylation to gene delivery efficiency. From Fig. 2E, we see that regardless of the PEG size, 100% PEGylated peptide/pDNA complexes showed zero transfection activity. When decreasing PEGylated peptide content in complexes, transfection ability was restored in a concentration dependent manner (Fig. 2E, 2-way ANOVA "PEGylation rate" $F(6, 123) = 14.53$, $p < .0001$).

In conclusion, complex formation and characterization studies showed that PEGylated analogs of PF14 were able to incorporate and condense pDNA into complexes and that simply mixing the parent PF14 with PEGylated peptides is an effective, simple, and flexible approach to prepare noncovalent functionalized CPP/nucleic acid complexes at any PEGylation rate, yielding complexes that are both stable and retain the ability to partially release pDNA. Finally, PEG as a shield has a potential to mask transfection ability of PF14.

3.2.3. The resistance of PEGylated peptide/pDNA complexes to degradative enzymes

One requirement for gene delivery vectors is to protect their cargo from degradative enzymes such as nucleases and proteases. To assess these properties we analyzed serum treated particles with gel shift assay and subsequently evaluated their transfection ability in cells to determine how much transfection efficiency remained. Not surprisingly, we saw that naked pDNA is susceptible to serum degradation but complexation with PF14 is able to protect pDNA, at least partially (Fig. S4A, B). Similar pDNA protective effect was seen when small amount (10% and 20%) of PF14 was substituted with PEGylated peptides (Fig. S4A, B).

We next transfected cells with the serum treated complexes. Not surprisingly, PF14/pDNA complexes were resistant to serum degradative enzymes (Fig. S4C) even after 4 h of incubation with FBS (Fig. S4D). However, PEGylated complexes were less efficient in transfection efficacy (Fig. S4C and D). We replicated similar in vitro stability tests using higher PEGylation rate (40%) and a more straightforward assay with nuclease, DNase I. As expected, all of the free pDNA was degraded by the nuclease treatment (Fig. 3A). At CR2, PF14 and PEG-PF14 protected pDNA to a small extent. Using peptides at CR4 offered more efficient protection against the nuclease activity, especially in the case of PF14 and PF141 (Fig. 3A). Finally, when cells were transfected with the DNase pretreated complexes, neither PF14 nor PEG-PF14 were affected by the nuclease treatment (Fig. 3B). To sum up, compared to PF14/pDNA complexes, formulations with PEGylated peptides seem to be slightly less stable according to DNA protection ability and transfection efficacy after degradative challenge. Although these results suggest smaller complex stability in degradative environment, it does not exclude the possibility that slightly decreased stability in such environments could contribute higher gene induction. Also, there are other important factors that determine in vivo efficacy, such as potential aggregation and immune activation.

3.2.4. Characterization of PEGylated peptide/pDNA complexes in vivo

Next we tested the efficacies of PEGylated complexes in vivo conditions. Firstly we determined the availability of nanocomplexes after 24 h of administration, for that the biodistribution of PF14/pDNA and PEGylated PF14/pDNA complexes were evaluated. We complexed Cy5-labeled pDNA with the peptides and analyzed the fluorescence content in different tissues. Prior to administration we assessed if Cy5-

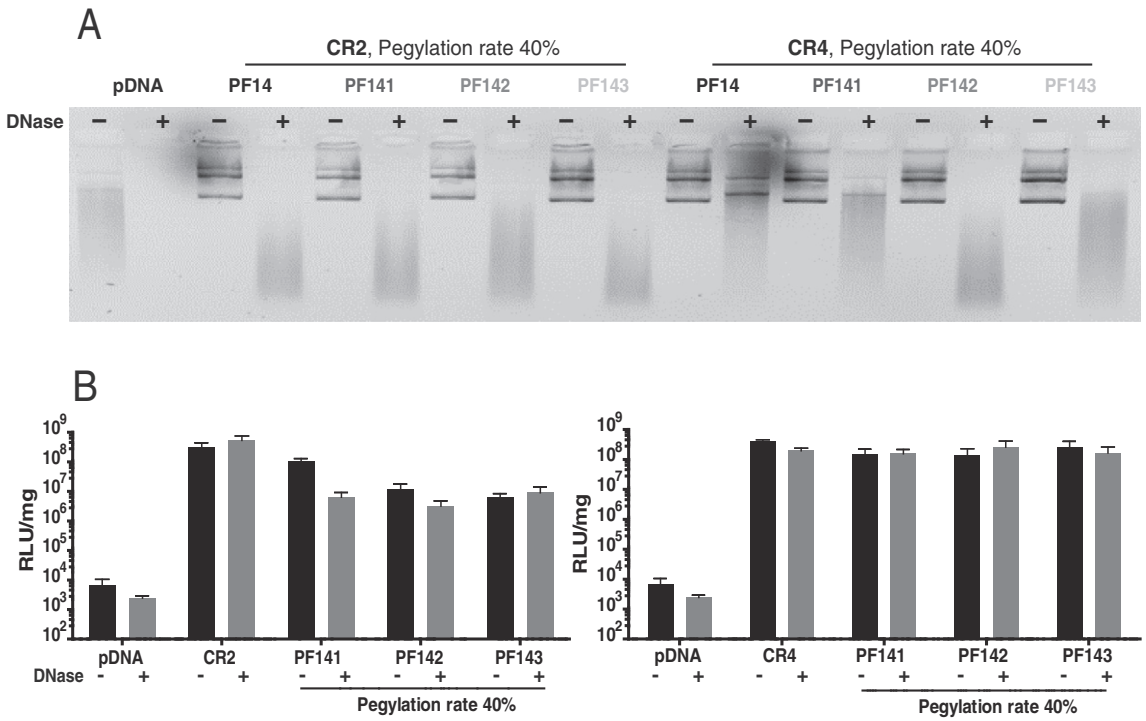

Fig. 3. The ability of complexes to protect pDNA from nucleases. (A) Preformed complexes (at CR2 and CR4) with PF14 or PEGylated peptides (PEGylation rate 40%) were incubated with DNase for 30 min. To visualize pDNA degradation, peptides in all complexes and naked pDNA control were digested using proteinase K and thereafter pDNA was visualized using a gel shift assay. CHO cells were transfected with DNase treated PF14/pDNA or 40% of PEGylated complexes made at CR2 (B) and CR4 (C). 24 h later, cells were lysed and luciferase activity was measured and normalized against protein content.

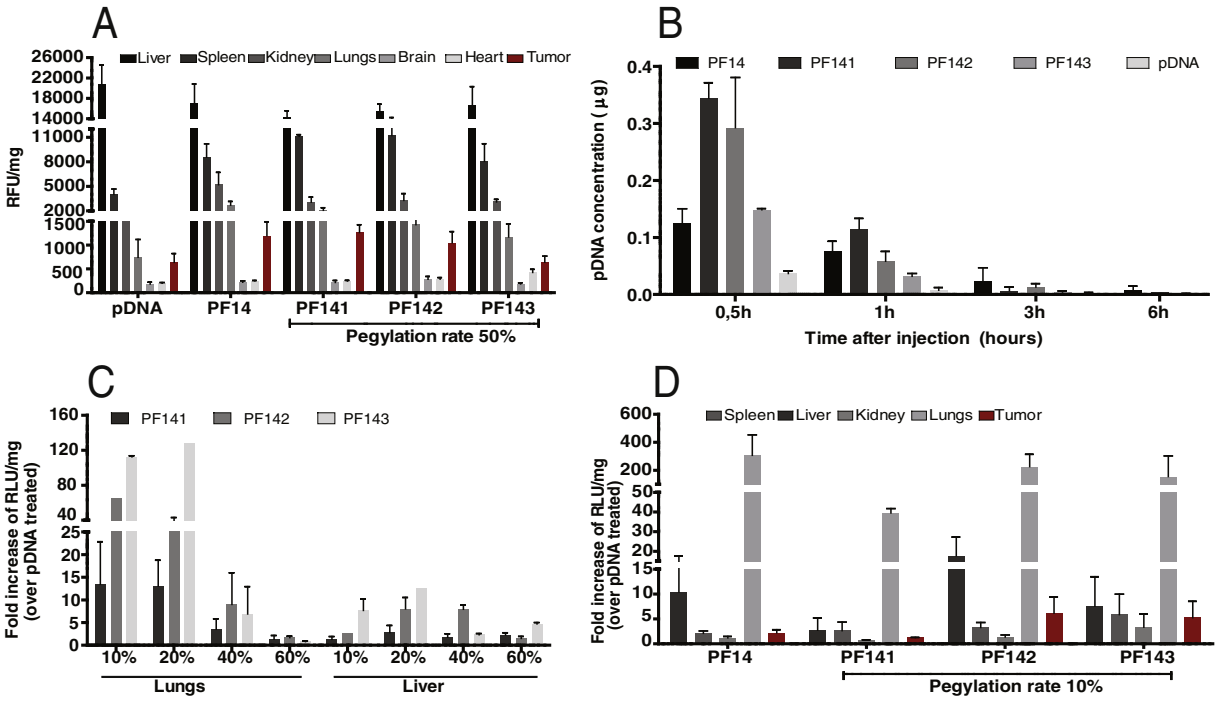

Fig. 4. In vivo characterization of PEGylated PF14 complexes with pDNA. To assess the biodistribution of PEGylated nanocomplexes (A) and complex stability in blood (B), Cy5 labeled pDNA (20 µg) was mixed with peptides at CR4, using PEGylation rate 50%. Blood was collected at specified time points and tissues were collected after 24 h. Obtained fluorescence values from tissues were normalized against the protein content. (C) To evaluate the impact of the PEGylation rate of complexes to induce gene expression levels in the lungs and liver, complexes with PF141, PF142, PF143 and pLuc2 (CR4, 20 µg) were formed at different PEGylation rates ranging from 10% to 60% and administrated i.v. 24 h later, tissues were harvested and luciferase activity was measured and normalized to protein content. Data is represented as fold increase of RLU/mg over pDNA treated group. N = 4 in each group. (D) To compare the ability to induce gene expression in different organs and U87 tumors, PF14/pDNA and PEGylated peptide/pDNA complexes were formed (PEGylation rate 10%, CR4, 20 µg pDNA), administered i.v. and 24 h luciferase activity was measured from the tissues as described above. N = 3–6 in each group.

labeled pDNA was incorporated into complexes similarly to normal pDNA and confirmed no major differences (Fig. S5A–C). The only observed difference was that PF142 and PF143 complexes with Cy5-pDNA dissociated less in the presence of the highest concentration of heparin, a possible modulating effect to hydrophobicity of the Cy5 dye. Nevertheless, both the modified and unmodified pDNA were incorporated into similar complexes. After administration of complexes it was seen clearly that PEGylation altered biodistribution of the complexes. While not surprising, complexation of pDNA with PF14 enriches the signal in the lungs (as also suggested by their ability to induce *luc* gene in the lungs), the complexes with PF142 and PF143 showed markedly lower lung accumulation (Fig. 4A). Secondly, PEGylation seems to increase their distribution in other tissues. We hypothesize that PEGylation could reduce complex accumulation in lung tissue and therefore they are more available to other tissues. For example, compared with PF14/pDNA complexes, PEGylation increased the accumulation of complexes in the spleen and heart (Fig. 4A). To assess the pharmacokinetic effect of PEGylation, Cy5-pDNA levels in blood was measured at several time points after the injection. As can be seen in Fig. 4B, naked pDNA is cleared already 1 h postinjection, while the CPP-complexed pDNA persists for 3 h ($p < .01$, Tukey post-hoc pDNA group versus PF141 or PF142, ANOVA $F(10, 71) = 2.89$, $p < .01$). Moreover, PEGylation further decreases the rate of elimination, because the levels of PEGylated pDNA/PF14 complexes reach up to 2 times higher, compared with complexes without PEG ($p < .011$, Tukey post-hoc PF141 group versus PF14). This suggests that functionalization of complexes with PEG inhibits their contact with blood serum elements, and/or PEGylation inhibits high lung accumulation, resulting in a longer circulation half-life.

We characterized the ability of PEGylated peptide/pDNA complexes to induce gene expression using PEGylation rates from 10% to 60% and CR4. As with the in vitro experiments, the aim was to titrate PEGylation rate and assess its inhibiting effect on gene induction. We observed that PF141 (PEG600) was less efficient in gene induction compared with either PF142 (PEG1000) or PF143 (PEG2000) (Fig. 4C). For all the peptides, increasing the PEG content gradually decreased gene expression levels in the lungs, reaching the zero level at 60% PEGylation rate. PEG shielding effect is apparent and in accordance with in vitro transfection profiles. The smaller efficacy of PF141 could be caused by less stable complexes. Particle characterization (Fig. 2) showed that PEG600 in PF141 results in more loose complexes, compared with larger PEG analogs. Importantly, none of the PEGylated PF14/pDNA complexes exhibited the occasional toxicity that we observed in the case of non-PEGylated particles, further favoring their in vivo use.

An obvious question when adding a PEG shield to a delivery vector is: How does this influence temporal gene induction? Accordingly, PEG may well prolong the complex circulation time and gene induction may be induced at a later time point. We therefore assessed the induction of the *luc* gene at a later time point. Nevertheless, this proved not to be the case, because the gene expression levels with or without PEG showed a similar decline in time, and in both cases *luc* expression levels returned to baseline within 48 h after the injection (Fig. S6A–B). Nevertheless, the gene induction efficacy depends on both the delivery efficacy and the properties of the expression vector. Thus, conclusive remarks can be drawn after assessing the influence of pDNA elements such as the presence of a CMV promoter [19], CpG patterns [20], etc.

These observations support our initial hypothesis that PEG is able to form a shielding barrier between the active core and outer environment (Fig. 1C), thereby providing advantages that are crucial for in vivo applications. Pegylation increases blood circulation half-life (Fig. 4B), which can be used to yield a more favorable delivery efficacy. It may also provide protection from immune system recognition and subsequent unfavorable reactions. Indeed, we did not observe any toxic reactions with any of the PEGylated PF14/pDNA particles. Second, PEGylation inactivates the high transfection ability of PF14, which may seem to be a contradictory goal when developing an efficient delivery vector. However, PEG can be conjugated via small and functional linkers that can be cleaved upon fulfillment of certain environmental criteria, such as in the presence of tumor-specific extracellular proteases [21], which could allow for controllable gene induction specifically in tumors.

3.3. Construction of tumor-sensitive pDNA delivery vector

3.3.1. Passive accumulation of peptide/pDNA complexes in tumors

Because our goal was to develop a tumor-activatable gene delivery platform, we first assessed the behavior of the unmodified parent CPP. Therefore, we investigated if PF14/pDNA complexes were able to passively accumulate inside tumors and induce gene expression. For that we induced subcutaneous tumors from human glioblastoma cell line U87. We observed that PF14/pDNA complexes were not able to trigger significant gene expression in tumors (Fig. 4D) 24 h postinjection, although the complexes are able to transfect cells in vitro [14]. We speculate that PF14/pDNA complexes are quickly cleared from blood circulation and therefore are not passively accumulating in tumors and could not be taken up by tumor cells. In addition, PF14/pDNA complexes displayed more gene induction in the lungs (Fig. 1A) where luciferase expression was at least 10 times higher than in other tissues. It may be that the majority of complexes are rapidly taken up by the lungs and thus interfere with passive accumulation within tumors.

The PF14/pDNA complexes failed to accumulate to tumors and displayed high gene induction in the lungs, whereas the PEGylated complexes displayed altered biodistribution (Fig. 4A) and prolonged circulation time (Fig. 4B). Therefore, our hypothesis was that these particles could passively accumulate in tumors through the EPR effect. Indeed, we observed that adding PEG prevented high lung gene induction, while at the same time possibly even enhancing gene induction in other organs (Fig. 4C). We therefore assessed the gene delivery efficacy of CPP-PEG in U87 tumor bearing mice. Intriguingly, even a 10% PEGylation rate induced significant gene expression in tumors, reaching up to 7-fold over pDNA treatment (Fig. 4D). We decided that it is suitable to proceed with tumor-specific targeting and add further modifications to the characterized PEGylated PF14 analogs.

3.3.2. Construction of MMP2-sensitive particles

Next, we reasoned that if PEGylation of the complexes enables us to decrease PF14 gene induction in the lungs and improve tumor delivery (Fig. 4D), the tumor specificity could potentially be increased if a tumor-specific cleavable linker were introduced between PEG and CPP moieties (Fig. 1C). Conceivably, a combination of higher PEGylation rate and cleavable PEG in complexes would inhibit general uptake in tissues and provide tumor-specific gene induction. In this way the particle properties would depend on the conditions of the extracellular environment and PEG could be removed after passive accumulation near tumor cells, thereby enhancing specific gene induction. The tumor-specific environmental conditions could be pH [22] or temperature [23]. However, there are several successful reports on carriers that depend on tumor-specific enzymatic cleavage [21,24]. Therefore, we introduced an extra MMP2-cleavable linker to PEGylated PF14 analogs (Table 1) and assessed their tumor-specific gene induction. PEG moieties with different molecular weights were covalently attached to the C-terminal end of PF14 peptide through an MMP2-cleavable sequence [11]. A scrambled MMP2 cleavable sequence was used as a negative control. A PEGylation rate of 50% was chosen because at this rate transfection efficiency was entirely masked in vitro (Fig. 2E); however, complexes still formed and pDNA was condensed (Figs. 2, S3). Furthermore, at 50% PEGylation, in vivo, gene induction was inhibited for all PEG sizes (Fig. 4C).

To validate MMP2 enzyme cleavability, peptides were digested with recombinant MMP2 enzyme and thereafter analyzed by RP-UPLC. Chromatograms showed that near complete cleavage was accomplished

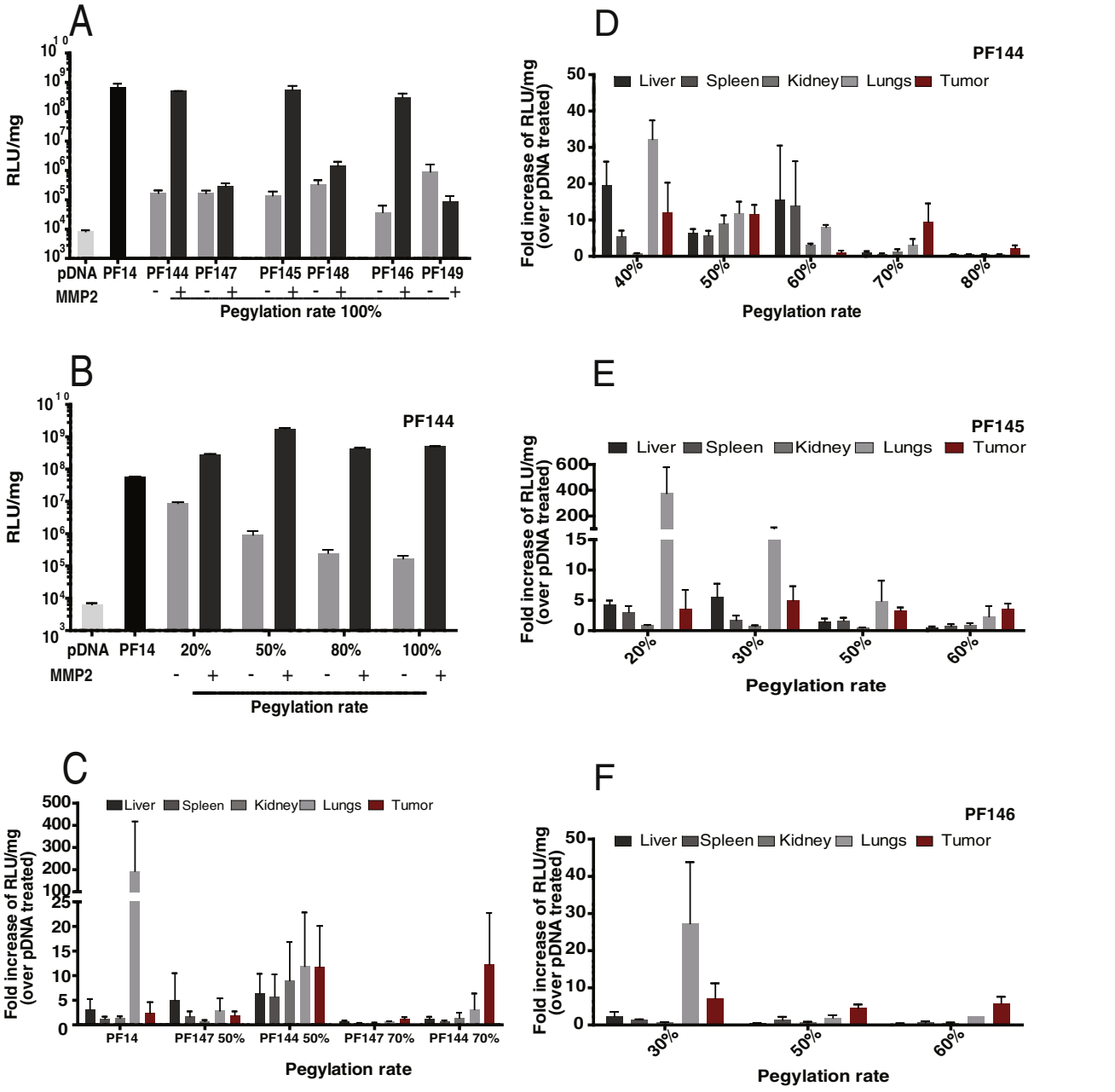

Fig. 5. Biological activity of PEGylated MMP-sensitive peptide/pDNA complexes. (A) Peptide/pDNA complexes at CR2 were preincubated with active recombinant MMP2 (0.1 mg/ml) for 30 min at 37 °C and thereafter delivered in U87 cells. 24 h after transfection luciferase activity was measured and normalized against protein content. (B) The transfection efficiency of MMP2-sensitive PF144/pDNA complexes at PEGylation rates of 20%, 50%, 80% and 100% was evaluated using U87 cells. For that all complexes were preincubated with MMP2 and luciferase activity was analyzed as described above. (C) The ability of PF147, PF144 and pDNA complexes to induce gene expression in different tissues and subcutaneous Neuro2a tumors was evaluated. For that, peptide/pDNA (CR4, 20 μg) complexes were formed at the PEGylation rate of 50% or 70%. Complexes were administered i.v. via the tail vein. 24 h later, tissues were harvested and luciferase activity was measured and analyzed as described earlier. N = 4–6 in each group. The ability of (D) PF144, (E) PF145 and (F) PF146 complexes at different PEGylation rates to induce gene expression in different tissues and subcutaneous Neuro2a tumors was evaluated. For that, peptide/pDNA (CR4, 20 μg) complexes were formed at PEGylation rates of 20–80%. N = 3–4 in each group.

after 40 min of incubation in the case of PF144 (cleavable PEG600) while the peak of PF147 (uncleavable PEG600) did not disappear after MMP2 digestion (Fig. S7).

Thereafter we conducted experiments first in cell culture, using Neuro2a and U87 cell lines, comparing the MMP2 sensitive PEGylated peptides with their respective uncleavable peptides. To assess the effect of MMP2 activation on transfection, the complexes were preincubated with the MMP enzyme. Consistent with our hypothesis, MMP-treated complexes were able to induce gene expression levels comparable to that of PF14/pDNA in U87 cells (Fig. 5A), while the complexes not incubated with the enzyme did not induce significant gene expression, similar to complexes made with uncleavable peptides. Similar results were obtained in Neuro2A cells (Fig. S8C). We also verified that neither the PEGylated peptides nor MMP2 enzyme induced toxic effects on the cells by carrying out a cell viability assay (Fig. S8A, B). We next titrated the PEG% in MMP2-sensitive complexes and observed that regardless of the PEGylation rate, the efficacy of the preactivated complexes reached at least the same levels as PF14/pDNA (Fig. 5B). In the case of 50% PEG in PF144, the gene expression levels were even one log higher. It seems that PEGylation does not hinder the accessibility of MMP2 enzyme (at least in vitro), which is important for tumor-specific activation of these complexes. Nevertheless, we hypothesize that in vivo MMP2

levels are much lower than the level used here (even in highly malignant tumors) and increasing the PEGylation rate could decrease efficacy due to insufficient activation by the protease.

We proceeded with a 50% PEGylation rate, using PF144/PF14 complexes for in vivo evaluations. Accordingly, reporter gene expression was greatly reduced in the lungs, yet significantly increased in Neuro2a tumors at 50% PEGylation (Fig. 5C). Furthermore, increasing PEGylation rate up to 70% permitted gene induction specifically in tumors, leaving luciferase levels to baseline in other organs (Fig. 5C). Selective gene expression in tumors is probably mediated by sufficient masking of CPP activity via increasing PEGylation rate of complexes and tumor sensitive induction of gene expression is achieved via specific CPP/pDNA complex activation after removal of PEG by MMP2 cleavage. This expression profile encouraged us to assess the gene induction mediated by the cell-penetrating peptides carrying increasing size of PEGs (Table 1).

We demonstrate that it is possible to enhance or inhibit gene expression in different organs according to necessity, by using different PEGylation rates (Fig. 5D–F). For example using PF145 (PEG1000) or PF146 (PEG2000) at lower PEGylation rates enables to reduce gene expression levels to baseline levels, at the same time inducing high gene expression in the lungs. On the other hand, PF144 at PEGylation rate 50% is able to induce uniform gene expression in organs and Neuro2a tumor (Fig. 5D). Nevertheless, it should be noted that MMP-sensitive activation depends on MMP levels in particular tumor, i.e. tumor growth aggressiveness. Therefore, the PEGylation rate should be optimized for different types of tumors. To summarize, applying this strategy enables specific and flexibly adjustable induction of gene expression in different organs and tumors, therefore representing simple and efficient gene delivery platform for therapeutic interventions.

4. Conclusions

In conclusion, we propose a simple method to functionalize noncovalent CPP/nucleic acid complexes. As a proof of concept, we have utilized this strategy for obtaining a tumor-selective gene delivery vector and effectively induced expression of a reporter gene in tumor tissues. Importantly, this approach may be extended to other CPPs and include other types of functional moieties due to the simple flexible formulation and functionalization of nucleic acid and CPP complexes.

Acknowledgment

We thank M. Hallbrink and M. Pooga for the insightful ideas and guidance.

This work was supported by EU through the European Regional Development Fund through the project Tumor-Tech (3.2.1001.11-0008) and the Centre of Excellence of Chemical Biology (3.2.0101.08-0017), by the Estonian Ministry of Education and Research through IUT20–26, by Swedish Research Council (VR-NT) and the Swedish Cancer Foundation.

Appendix A. Supplementary data

Supplementary data to this article can be found online at http://dx.doi.org/10.1016/j.jconrel.2015.04.038.

References

[1] E. Wagner, Polymers for siRNA delivery: inspired by viruses to be targeted, dynamic, and precise, Acc. Chem. Res. 45 (2012) 1005–1013, http://dx.doi.org/10.1021/ar2002232.
[2] J. Suhorutsenko, N. Oskolkov, P. Arukuusk, K. Kurrikoff, E. Eriste, D.-M. Copolovici, et al., Cell-penetrating peptides, pepFects, show no evidence of toxicity and immunogenicity in vitro and in vivo, Bioconjug. Chem. 22 (2011) 2255–2262, http://dx.doi.org/10.1021/bc200293d.
[3] M. Kullberg, R. McCarthy, T.J. Anchordoquy, Systemic tumor-specific gene delivery, J. Control. Release 172 (2013) 730–736, http://dx.doi.org/10.1016/j.jconrel.2013.08.300.
[4] W. Zhang, Q. Cheng, S. Guo, D. Lin, P. Huang, J. Liu, et al., Gene transfection efficacy and biocompatibility of polycation/DNA complexes coated with enzyme degradable PEGylated hyaluronic acid, Biomaterials 34 (2013) 6495–6503, http://dx.doi.org/10.1016/j.biomaterials.2013.04.030.
[5] J. Wang, Y. Lei, C. Xie, W. Lu, E. Wagner, Z. Xie, et al., Retro-inverso CendR peptide-mediated polyethyleneimine for intracranial glioblastoma-targeting gene therapy, Bioconjug. Chem. 25 (2014) 414–423, http://dx.doi.org/10.1021/bc400552t.
[6] Ü. Langel (Ed.), , Cell-penetrating peptides, Humana Press, Totowa, NJ, 2011 (http://link.springer.com/10.1007/978-1-60761-919-2 (accessed July 7, 2014)).
[7] T. Lehto, O.E. Simonson, I. Mäger, K. Ezzat, H. Sork, D.-M. Copolovici, et al., A peptide-based vector for efficient gene transfer in vitro and in vivo, Mol. Ther. 19 (2011) 1457–1467, http://dx.doi.org/10.1038/mt.2011.10.
[8] M.C. Morris, P. Vidal, L. Chaloin, F. Heitz, G. Divita, A new peptide vector for efficient delivery of oligonucleotides into mammalian cells, Nucleic Acids Res. 25 (1997) 2730–2736, http://dx.doi.org/10.1093/nar/25.14.2730.
[9] K. Rittner, A. Benavente, A. Bompard-Sorlet, F. Heitz, G. Divita, R. Brasseur, et al., New basic membrane-destabilizing peptides for plasmid-based gene delivery in vitro and in vivo, Mol. Ther. 5 (2002) 104–114, http://dx.doi.org/10.1006/mthe.2002.0523.
[10] T. Jiang, E.S. Olson, Q.T. Nguyen, M. Roy, P.A. Jennings, R.Y. Tsien, Tumor imaging by means of proteolytic activation of cell-penetrating peptides, Proc. Natl. Acad. Sci. U. S. A. 101 (2004) 17867–17872, http://dx.doi.org/10.1073/pnas.0408191101.
[11] A. Talvensaari-Mattila, P. Pääkkö, T. Turpeenniemi-Hujanen, Matrix metalloproteinase-2 (MMP-2) is associated with survival in breast carcinoma, Br. J. Cancer 89 (2003) 1270–1275, http://dx.doi.org/10.1038/sj.bjc.6601238.
[12] L. Zhu, T. Wang, F. Perche, A. Taigind, V.P. Torchilin, Enhanced anticancer activity of nanopreparation containing an MMP2-sensitive PEG-drug conjugate and cell-penetrating moiety, Proc. Natl. Acad. Sci. (2013)http://dx.doi.org/10.1073/pnas.1304987110 (201304987).
[13] M.L. Immordino, F. Dosio, L. Cattel, Stealth liposomes: review of the basic science, rationale, and clinical applications, existing and potential, Int. J. Nanomedicine 1 (2006) 297–315.
[14] K.-L. Veiman, I. Mäger, K. Ezzat, H. Margus, T. Lehto, K. Langel, et al., PepFect14 peptide vector for efficient gene delivery in cell cultures, Mol. Pharm. 10 (2013) 199–210, http://dx.doi.org/10.1021/mp3003557.
[15] M. Manthorpe, F. Cornefert-Jensen, J. Hartikka, J. Felgner, A. Rundell, M. Margalith, et al., Gene therapy by intramuscular injection of plasmid DNA: studies on firefly luciferase gene expression in mice, Hum. Gene Ther. 4 (1993) 419–431, http://dx.doi.org/10.1089/hum.1993.4.4-419.
[16] J.W. McLean, E.A. Fox, P. Baluk, P.B. Bolton, A. Haskell, R. Pearlman, et al., Organ-specific endothelial cell uptake of cationic liposome-DNA complexes in mice, Am. J. Physiol. Heart Circ. Physiol. 273 (1997) H387–H404.
[17] P. Chollet, M.C. Favrot, A. Hurbin, J.-L. Coll, Side-effects of a systemic injection of linear polyethylenimine–DNA complexes, J. Gene Med. 4 (2002) 84–91, http://dx.doi.org/10.1002/jgm.237.
[18] S.-J. Sung, S.H. Min, K.Y. Cho, S. Lee, Y.-J. Min, Y.I. Yeom, et al., Effect of polyethylene glycol on gene delivery of polyethylenimine, Biol. Pharm. Bull. 26 (2003) 492–500, http://dx.doi.org/10.1248/bpb.26.492.
[19] R. Scharfmann, J.H. Axelrod, I.M. Verma, Long-term in vivo expression of retrovirus-mediated gene transfer in mouse fibroblast implants, Proc. Natl. Acad. Sci. 88 (1991) 4626–4630.
[20] H. Hemmi, O. Takeuchi, T. Kawai, T. Kaisho, S. Sato, H. Sanjo, et al., A Toll-like receptor recognizes bacterial DNA, Nature 408 (2000) 740–745, http://dx.doi.org/10.1038/35047123.
[21] E.S. Olson, T.A. Aguilera, T. Jiang, L.G. Ellies, Q.T. Nguyen, E.H. Wong, et al., In vivo characterization of activatable cell penetrating peptides for targeting protease activity in cancer, Integr. Biol. Quant. Biosci. Nano Macro 1 (2009) 382–393, http://dx.doi.org/10.1039/b904890a.
[22] H. Wu, L. Zhu, V.P. Torchilin, pH-sensitive poly(histidine)-PEG/DSPE-PEG co-polymer micelles for cytosolic drug delivery, Biomaterials 34 (2013) 1213–1222, http://dx.doi.org/10.1016/j.biomaterials.2012.08.072.
[23] G. Li, Y. Meng, L. Guo, T. Zhang, J. Liu, Formation of thermo-sensitive polyelectrolyte complex micelles from two biocompatible graft copolymers for drug delivery, J. Biomed. Mater. Res. A 102 (2014) 2163–2172, http://dx.doi.org/10.1002/jbm.a.34894.
[24] M. Mäe, O. Rautsi, J. Enbäck, M. Hällbrink, K.R. Aizman, M. Lindgren, et al., Tumour targeting with rationally modified cell-penetrating peptides, Int. J. Pept. Res. Ther. 18 (2012) 361–371, http://dx.doi.org/10.1007/s10989-012-9312-1.